MULTIPARAMETRIC MRI ASSESSMENT OF NECROTIC EPIPHYSEAL CARTILAGE INDUCED BY TRANSECTION OF CARTILAGE CANAL BLOOD VESSELS IN GOAT KIDS

Luning Wang[1], Mikko J Nissi[2], Ferenc Toth[3], Michael Garwood[1], Cathy Carlson[3], and Jutta Ellermann[1]

[1]*Center for Magnetic Resonance Research, University of Minnesota, Twin Cities, Minneapolis, MN, United States,* [2]*Medical Research Center Oulu, Oulu University Hospital and University of Oulu, Finland,* [3]*University of Minnesota, Twin Cities, Minneapolis, MN, United States*

Target Audience: Scientists and clinicians interested in cartilage imaging, relaxation time mapping, novel pulse sequences, osteochondritis dissecans.

Purpose: Juvenile Osteochondritis Dissecans (OCD) is a poorly understood disease of children and young adults that may be associated with significant lifelong disability. The role of changes occurring in the epiphyseal cartilage matrix, likely related to ischemic vascular events affecting the developing skeleton, is poorly understood. Previous cartilage research has been focused almost entirely on the avascular articular cartilage [1]. Our goal is to probe the utility of noninvasive parametric MRI methods in an animal model to better understand the etiology of developmental orthopaedic diseases in children and adolescents, such as juvenile osteochondritis dissecans (OCD). Here, we present relaxation time mapping of surgically-induced ischemia in the femoral condyle of goats at different stages of lesion development which are similar to those identified in the early stages of development of naturally-occurring OCD. T_1, T_2, continuous wave (CW) $T_{1\rho}$ and adiabatic $T_{1\rho}$ relaxation times [2] as well as the relaxation along a fictitious field (T_{RAFF}) [3] were acquired, tested for their ability to detect the area of ischemic necrosis of cartilage, and compared with semi-quantitative histology.

Methods: Distal femoral epiphyseal specimens were obtained from goats in that had undergone surgical transection of cartilage canal blood vessels in the medial condyle at 4 days of age. Goats were euthanized 4, 6, and 10 weeks after surgery [4]. Respective parametric MR relaxation time mapping of the specimens was performed using a 9.4T Varian scanner (Agilent Technologies, Santa Clara, CA). The MR imaging parameters are detailed in Table 1. Optical density measurements of Safranin O stained histologic sections matching the MRI slices of the knees was done to assess proteoglycan (PG) loss in areas of ischemic cartilage necrosis [5].

Results: Safranin O stained sections depicted areas of focal loss of staining within the intensely stained epiphyseal cartilage (first row in Figure 1, arrows). The optical density measurements in the corresponding Safranin O stained sections (second row in Figure 1) indicated that the focal loss of stain was due to PG loss in area of necrosis. All of the relaxation parameters were able to differentiate between articular and epiphyseal cartilage, as well as between the ischemic lesion and the normal surrounding epiphyseal cartilage (Figure 2, arrows). Relaxation times were consistently higher in articular than in epiphyseal cartilage (Table 2). In the early development of the lesion, the T_2 relaxation time decreased approximately 16% from 4 to 6 weeks after lesion induction, which is the largest change of all of the relaxation times. The adiabatic and CW $T_{1\rho}$ relaxation times had the most striking changes later in the disease process, as PG loss became more dramatic in the necrotic cartilage. T_{RAFF} demonstrated sensitivity to the difference between the necrotic and normal epiphyseal cartilage at both the early and late stages of the disease.

Discussion: T_2 is suitable for detecting necrosis at the early stage of OCD, while adiabatic and CW $T_{1\rho}$ perform better at later stages. The adiabatic $T_{1\rho}$, by the use of adiabatic pulses, should be more robust against B0 and B1 variations than the CW $T_{1\rho}$ and having similar diagnostic performance is the preferred method of the two. Compared to other methods, T_{RAFF} appeared to have a higher sensitivity to the lesion at all stages, likely because T_{RAFF} is influenced by both $T_{1\rho}$ and $T_{2\rho}$ relaxations, making it sensitive to various biological changes. Thus far, there are no publications indicating which chemical compounds affect T_{RAFF} in the epiphyseal cartilage. However, this work demonstrated that the T_{RAFF} relaxation time of both necrotic and healthy epiphyseal cartilage changed as the animal aged, indicating that proteoglycans and likely also collagen contribute to the variation of T_{RAFF}. More specifically, at the early stages of OCD, T_{RAFF} is potentially influenced more by the $T_{2\rho}$ component, while at the later stages, the $T_{1\rho}$ component could become more important as indicated by the changes in the other relaxation parameters. Because it is influenced by several chemical compounds simultaneously, T_{RAFF} is a unique and robust parameter for detecting OCD-related changes. Another advantage of RAFF is that, compared to CW pulses, it implements the amplitude modulation to reduce about 40% SAR while providing the same duration and B_1^{max} setting [2].

Conclusion: The measurement of various MRI relaxation times provided a sensitive, noninvasive way to detect ischemic necrosis of the epiphyseal cartilage in a goat model of osteochondritis dissecans. While the T_2 relaxation time revealed very early cartilage matrix changes after transection of cartilage canal blood vessels, both CW and adiabatic $T_{1\rho}$ were more sensitive to later changes associated with proteoglycan loss. T_{RAFF} relaxation time combined sensitivity to both early and later stages of the disease. For future studies on children with OCD these noninvasive measurement methods are promising for staging of the disease and for outcome measures following intervention.

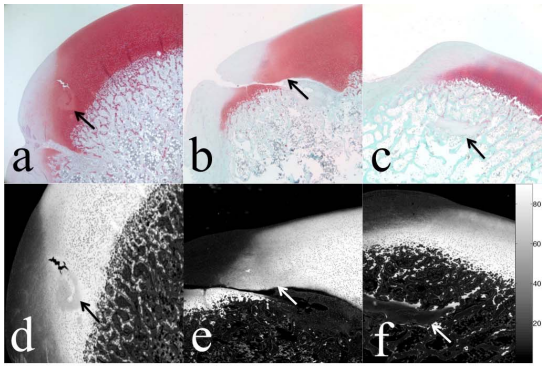

Figure 1. Safranin-O staining was used to demonstrate proteoglycan loss in the epiphyseal cartilage at (a) 4, (b) 6 and (c) 10 weeks post surgery. The second row shows the absorption of the 530 nm light by the Safranin-O stain. Both the focal loss of stain in the first row and the decreased light absorption in the second row (indicated by arrows) indicate a reduction of proteoglycan content within the area of surgically-induced ischemic necrosis, compared to the normal epiphyseal cartilage

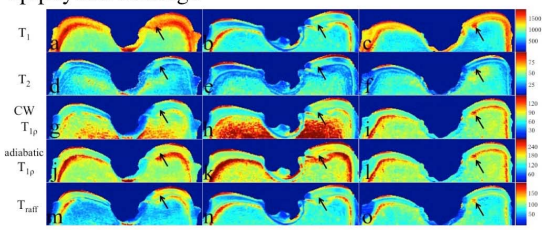

Figure 2. This figure shows the different relaxation times of the goat knees. Arrows indicate the regions of necrosis in the epiphyseal cartilage. The first to the third columns correspond to 4, 6, and 10 weeks post-surgical time points.

Table 1. MRI sequences and parameters

FSE Readout	TR = 5s, ETL = 8, thk = 1 mm, FOV = 4 cm, 256 × 256, coronal
T_1	IR, TI = 0.07, 0.08, 0.1, 0.16, 0.32, 0.64, 1.28, 2.56, 5.12 s, TE = 10 ms
T_2	Double spin echo preparation, T = 4, 20, 40, 60, 80, and 100 ms, TE = 10 ms
CW $T_{1\rho}$	γB_1^{max} = 500 Hz, T = 0, 10, 20, 40, and 80 ms, TE = 10 ms
Adiabatic $T_{1\rho}$	Train of 0, 4, 8, 12, 16 AFP pulses, duration = 6 ms, γB_1^{max} = 2.5 kHz, TE = 10 ms
T_{RAFF}	Train of 0, 8, 16, 24, 32 RAFF pulse, duration = 4.53 ms, γB_1^{max} = 625 Hz, TE = 5 ms

Table 2. Relaxation times (mean ± SD) at different time points after the surgery

Time points	Tissue	T_1 [s]	T_2 [ms]	CW $T_{1\rho}$ [ms]	Adiabatic $T_{1\rho}$ [ms]	T_{RAFF} [ms]
4 weeks	Articular	1.62 ± 0.16	68.4 ± 15.9	95.2 ± 24.2	223.0 ± 48.3	175.7 ± 35.9
	Epiphyseal	1.34 ± 0.06	32.6 ± 8.7	57.2 ± 9.1	157.9 ± 16.2	100.8 ± 14.3
	Necrosis	1.38 ± 0.04	44.0 ± 3.4	64.4 ± 3.5	162.5 ± 10.4	126.4 ± 5.1
6 weeks	Articular	1.78 ± 0.24	84.8 ± 16.9	100.1 ± 21.6	283.2 ± 61.0	144.1 ± 28.4
	Epiphyseal	1.29 ± 0.04	22.8 ± 5.9	58.2 ± 4.3	147.9 ± 9.9	60.7 ± 9.6
	Necrosis	1.45 ± 0.05	46.1 ± 4.8	79.7 ± 3.7	181.7 ± 11.2	100.1 ± 7.1
10 weeks	Articular	1.58 ± 0.13	61.9 ± 10.0	85.7 ± 13.9	201.6 ± 37.0	134.4 ± 19.4
	Epiphyseal	1.27 ± 0.04	23.0 ± 5.9	53.5 ± 4.2	134.7 ± 9.6	69.0 ± 6.6
	Necrosis	1.56 ± 0.17	38.9 ± 18.4	128.5 ± 19.5	234.2 ± 35.4	137.3 ± 11.2

Acknowledgement: We grateful acknowledge the financial supports from NIH P41 EB015894 and R21 AR065385-01 grants and the WM KECK Foundation.

References: [1] Ellermann, J., et al. Magn Reson Imaging, 2013. **31**(9):1537-43. [2] Michaeli, S., et al. J Magn Reson, 2006. **181**(1):135-47. [3] Liimatainen, T., et al. Magn Reson Med, 2010. **64**(4):983-94. [4] Tóth, F. et al. Osteoarthritis and Cartilage. Accepted Manuscript: OAC1713R1. [5] Király, K., et al. Histochem J. 1996. 28(2):99-107.